Published in IET Signal Processing
Received on 20th March 2009
Revised on 20th October 2009
doi: 10.1049/iet-spr.2009.0067

Special Issue on Time-Frequency Approach to Radar Detection, Imaging, and Classification

ISSN 1751-9675

Space–time clutter rejection and target passive detection using the *APES* method

J. Raout[1] *A. Santori*[1] *E. Moreau*[2]

[1]*MorphoAnalysis in Signal Processing Laboratory, Research Center of the French Air Force, 13 661 Salon de Provence, France*
[2]*University of Sud Toulon Var, ISITV, LSEET UMR-CNRS 6017, av. G. Pompidou, BP 56, 83162 La Valette du Var, Cedex, France*
E-mail: jraout@sfr.fr

Abstract: A new method to reject ground clutter using the Amplitude and Phase EStimation (APES) method is proposed. The theoretical approach is followed by the application of this method to the rejection of such an interference in the frame of a bistatic passive radar using digital video broadcasting – terrestrial (DVB–T) transmitters.

1 Introduction

Radars using illuminators of opportunity are inherently passive bistatic radars. The passivity of bistatic radars offers definitive advantages namely low cost, low weight and enhanced radar cross-section for certain geometries. Moreover, stealth operations are possible since the receiver is totally passive.

Furthermore, noise-like signals allow unambiguous range and Doppler estimation and an independent control of Doppler and range measurements. Their ambiguity function presents no side lobes (just noise floor), and high rate compression is possible. In addition, they behave very favourably against electronic counter-measures (anti-radar missile and jamming). They also exhibit better performance in low probability of interception and exploiting. In the electromagnetic compatibility domain, better interference immunity and the possibility of using many radars simultaneously within the same area are expected.

Radars using illuminators of opportunity have already been studied. Signals provided by FM radio broadcast [1], satellites [2], digital video broadcasting-terestrial (DVB–T) [3] and global system for mobile communications (GSM) base stations [4] have been considered. Arguments for the selection of the transmitter type include spatial and time coverage, power, central-frequency and bandwidth of the emitted signal, and shape of the ambiguity function. The bandwidth dictates the achievable range-resolution and the shape of the ambiguity function is decisive in determining the detection performance of the radar. In particular, signals from digital modulation (GSM, DVB–T) have much less range and Doppler ambiguities than other modulations [5], which makes them more suitable for passive radar. In this paper, we will consider DVB–T transmitters as illuminators of opportunity. They have an ubiquitous spatial coverage, are permanent in time and have a thumbtack like ambiguity function because of the noise-like behaviour of the orthogonal frequency-division multiplexing (OFDM) modulation used.

Space–time adaptive processing (STAP) is typically used to filter out (clutter) interferences in GMTI radars in order to detect slow-moving targets. STAP offers a benefit over separate spatial and temporal processing when there is a coupling between the clutter signal direction of arrival and its Doppler frequency. STAP consists in performing a joint spatio-temporal optimum filtering of the signal in order to reject interference (clutter) contributions [6, 7].

Classical STAP methods such as the principal components method [7, 8], reduced rank methods such as the joint domain localised (JDL) method [8, 9] or the hybridisation of the JDL method with the direct data domain method [10–12] involve to estimate the covariance matrix of the interferences. Their performance can suffer from the presence of discrete sources of interference, the lack of homogeneous range cells for the estimation of the covariance matrix and the non-Gaussianity of the environment.

We propose in this paper not to use the covariance matrix but to iteratively reject components of the clutter using the Amplitude and Phase EStimation (APES) method [13–15].

Notations: *, ^{T}, †, $\hat{}$ represent, respectively, the conjugate, transpose, Hermitian transpose and estimate of a vector/matrix.

The element corresponding to the column c and row l of a matrix $\boldsymbol{M}$ will be represented by M_{lc}, its row index l by $\boldsymbol{M}_l$. The C first values of a vector $\boldsymbol{v}$ will be represented by $\boldsymbol{v}_C$, its lth element by v_l, the portion of this vector between elements i and j by $\boldsymbol{v}_{i:j}$.

The identity matrix with dimension N will be written as $\boldsymbol{I}_N$, $\boldsymbol{c}_C$ is the column vector with C unit elements, $\boldsymbol{0}_N$ the column vector with N null elements.

The Kronecker product is represented by $\otimes$, the Hadamard product by $\circ$. If we consider a $N \times M$ matrix $\boldsymbol{A}$, the vec-function of $\boldsymbol{A}$ is written vec($\boldsymbol{A}$) and is obtained by stacking the columns to obtain an $NM \times 1$ vector.

2 Signal model

Let us consider a sampled space–time signal $\boldsymbol{Y}$, made of clutter, potential target and noise, received by a sparse array antenna made of N_s elements, during a coherent integration time T_{ci} corresponding to N_d samples, so that $T_{ci} = N_d/f_s$, with f_s being the sampling frequency. The inter-element spacing between the $i+1$th antenna element and the previous one is represented by $d_{i+1,i}$ and the carrier wavelength by λ.

The various components of the received signal are defined by their amplitude, delay compared to the direct path, reduced Doppler frequency and associated steering vector in the temporal domain and direction of arrival linked to the steering vector in the spatial domain.

The general expression of a temporal steering vector in the direction of the reduced Doppler frequency $\nu_d = f_d/f_s$, with f_d the Doppler frequency is given by

$$\begin{aligned}\boldsymbol{s}_d(\nu_d) &= [1, e^{j2\pi\nu_d}, \ldots, e^{j2\pi\nu_d(N_d-1)}]^T \\ &= [1, z_d(\nu_d), \ldots, z_d^{N_d-1}(\nu_d)]^T \end{aligned} \quad (1)$$

where $z_d(\nu_d)$ stands for the temporal phase shift from one sample to another because of the motion of the considered component.

In the case of a sparse array (specifically used for real measurements presented in this paper), the spatial steering vector in the direction of arrival θ is

$$\begin{aligned}\boldsymbol{s}_s(\theta) &= \left[1, e^{j2\pi(\sin(\theta)/\lambda)d_{2,1}}, \ldots, e^{j2\pi(\sin(\theta)/\lambda)\sum_{i=0}^{N_s-1} d_{i+1,i}}\right]^T \\ &= \left[z_{s_{1,0}}(\theta), z_{s_{2,1}}(\theta), \ldots, \prod_{i=0}^{N_s-1} z_{s_{i+1,i}}(\theta)\right]^T \end{aligned} \quad (2)$$

where $z_{s_{i+1,i}}(\theta)$ stands for the spatial phase shift from the $i+1$th antenna element to the previous element. By convention, $z_{s_{1,0}}(\theta)$ is chosen equal to 1.

The space–time steering vector is deduced from both spatial and temporal steering vector

$$\boldsymbol{s}(\theta, \nu_d) = \boldsymbol{s}_d(\nu_d) \otimes \boldsymbol{s}_s(\theta) \quad (3)$$

The clutter signal $\boldsymbol{Y}_c$ is assumed to be made of the total contribution of N_r interfering range cells, creating multipaths. Each range cell is made of $N_{r,p}$ contributing clutter patches with complex amplitude $\alpha_{r,p}$, delay $\tau_r = r/f_s$, spatial steering vector $\boldsymbol{s}_s(\theta_{r,p})$ linked to the angle $\theta_{r,p}$. The internal clutter motion is also taken into account ($\nu_{d_{r,p}}$ is not necessarily equal to 0 and $\boldsymbol{s}_d(\nu_{d_{r,p}})$ is not necessarily equal to $\boldsymbol{c}_{N_d}$ $\forall r \in [1, \cdots, N_r]$ and $\forall p \in [1, \cdots, N_{r,p}]$) so that

$$\begin{aligned}\boldsymbol{Y}_c &= \sum_{r=1}^{N_r}\sum_{p=1}^{N_{r,p}} \boldsymbol{Y}_{c_{r,p}} \\ &= \sum_{r=1}^{N_r}\sum_{p=1}^{N_{r,p}} \alpha_{r,p}\boldsymbol{s}_s(\theta_{r,p})(\boldsymbol{x}(-\tau_r) \circ \boldsymbol{s}_d(\nu_{d_{r,p}}))^T \end{aligned} \quad (4)$$

with the general expression for the processed part of the reference signal

$$\boldsymbol{x}(-\tau_r) = \left[x\left(\frac{1-r}{f_s}\right), x\left(\frac{2-r}{f_s}\right), \ldots, x\left(\frac{N_d-r}{f_s}\right)\right]^T \quad (5)$$

The signal is also assumed to be made of the contribution of the target, $\boldsymbol{Y}_t$, that is, a signal with complex amplitude α and located at angle θ, reduced Doppler frequency ν_d and bistatic delay τ.

$$\begin{aligned}\boldsymbol{Y}_t &= \alpha\boldsymbol{s}_s(\theta)(\boldsymbol{x}(-\tau) \circ \boldsymbol{s}_d(\nu_d))^T \\ &= \alpha(\boldsymbol{c}_{N_s} \otimes \boldsymbol{x}^T(-\tau)) \circ (\boldsymbol{s}_s(\theta)\boldsymbol{s}_d^T(\nu_d)) \\ &= \alpha\boldsymbol{X}(-\tau) \circ (\boldsymbol{s}_s(\theta)\boldsymbol{s}_d^T(\nu_d)) \end{aligned} \quad (6)$$

Noise is represented by $\boldsymbol{N}$, an ergodic, stationary and zero mean random process. One can see in this model that clutter is considered as a finite sum of discrete contributors. Under this assumption, we propose to use a spectral estimation method, namely the APES method, to determine the amplitude, Doppler and angle of the main contributors and to subtract their contribution from the received signal, one after the other.

3 Generalisation of the APES method to noise-like signals

In the case of a bistatic radar exploiting a noise-like signal, a way to adapt the APES method [13–15] is to work on the mixing product defined for each range r associated to the

delay τ by

$$\boldsymbol{Y}_{\mathrm{m}}(\tau) = \boldsymbol{Y}(\tau) \circ (\boldsymbol{c}_{N_{\mathrm{s}}} \boldsymbol{x}^{\dagger}) \tag{7}$$

In an analog way, we will no longer consider the reference signal or the noise signal but their mixed version, $\boldsymbol{X}_{\mathrm{m}}$ and $\boldsymbol{N}_{\mathrm{m}}(\tau)$. Since the contributors induce a Doppler frequency that is much smaller than the sampling frequency, the signal can be low-pass filtered and subsampled as suggested in [16]. The subsampling factor will be denoted S. Note that this subsampling does not affect the range-resolution of the radar. The reduced Doppler frequency after this processing will be denoted $\tilde{\nu}_{\mathrm{d}} = \nu_{\mathrm{d}} S$. Low-pass filtering and subsampling play an important role in the adaptation of the APES method to noise-like signal. Both the demodulation of the received signal by the reference one (see (7)) and low-pass filtering plus subsampling allow the noise-like signal to get closer to a Doppler shifted pulse with a low level of amplitude fluctuations. This processing is associated to the subsampling and low-pass filtering matrix

$$\boldsymbol{S}(\nu_{\mathrm{d}}) = \mathrm{e}^{-\mathrm{j}\pi(S-1)\nu_{\mathrm{d}}} \frac{\sin(\pi\nu_{\mathrm{d}})}{\sin(\pi\tilde{\nu}_{\mathrm{d}})} \begin{bmatrix} \boldsymbol{c}_S & \boldsymbol{0}_S & \cdots & \cdots & \boldsymbol{0}_S \\ \boldsymbol{0}_S & \boldsymbol{c}_S & \boldsymbol{0}_S & \cdots & \boldsymbol{0}_S \\ \vdots & \ddots & \ddots & \ddots & \vdots \\ \vdots & \ddots & \ddots & \ddots & \vdots \\ \boldsymbol{0}_S & \cdots & \cdots & \boldsymbol{0}_S & \boldsymbol{c}_S \end{bmatrix}$$

$$= \iota(\nu_d) \boldsymbol{I}_{N_{\mathrm{d}}/S} \otimes \boldsymbol{c}_S \tag{8}$$

The correction by the coefficient $\iota(\nu_{\mathrm{d}}) = 1/\sum_{S-1}^{k=0} \mathrm{e}^{2\mathrm{j}\pi k\nu_{\mathrm{d}}}$ is necessary to compensate the effect of subsampling on the temporal steering vector. It yields

$$\boldsymbol{S}^{\mathrm{T}}(\nu_{\mathrm{d}}) \boldsymbol{s}_{\mathrm{d}}(\nu_{\mathrm{d}}) = \tilde{\boldsymbol{s}}_{\mathrm{d}}(\tilde{\nu}_{\mathrm{d}}) \tag{9}$$

The mixed signal defined in (7), for example, will now be replaced by

$$\begin{aligned} \tilde{\boldsymbol{Y}}(\tau, \nu_{\mathrm{d}}) &= \boldsymbol{Y}_{\mathrm{m}}(\tau) \boldsymbol{S}(\nu_{\mathrm{d}}) \\ &= \iota(\nu_{\mathrm{d}}) \boldsymbol{Y}_{\mathrm{m}}(\tau) \boldsymbol{S} \\ &= \iota(\nu_{\mathrm{d}}) \tilde{\boldsymbol{Y}}(\tau) \end{aligned} \tag{10}$$

One can see on the previous equation that it is not necessary to take into account a different mixed, low-pass filtered and subsampled signal $\tilde{\boldsymbol{Y}}(\tau, \nu_{\mathrm{d}})$ for each temporal direction but to work with $\tilde{\boldsymbol{Y}}(\tau)$ and to apply the correction. $\tilde{\boldsymbol{X}}$ and $\tilde{\boldsymbol{N}}(\tau)$ would be defined in the same way from $\boldsymbol{X}_{\mathrm{m}}$ and $\boldsymbol{N}_{\mathrm{m}}(\tau)$, respectively. The number of processed blocks, made of subsampled and low-pass filtered data, N_{d}/S will be denoted $\tilde{N}_{\mathrm{d}}$. Considering the mixed, low-pass filtered and subsampled signals, the purpose, for each step of the iterative rejection process, is to estimate the maximal amplitude $\hat{\alpha}_{r;\hat{p}}$ corresponding to the main contributor so that

$$\hat{\tilde{\boldsymbol{Y}}}_{c_{r;\hat{p}}}(\tau) = \hat{\alpha}_{r;\hat{p}} \tilde{\boldsymbol{X}} \circ (\boldsymbol{s}_{\mathrm{s}}(\theta_{r;\hat{p}}) \tilde{\boldsymbol{s}}_{\mathrm{d}}^{\mathrm{T}}(\tilde{\nu}_{\mathrm{d}_{r;\hat{p}}})) \tag{11}$$

For simplicity, the reference to the range cell (τ) and the spatio-temporal direction ($\theta_{r;\hat{p}}$, $\tilde{\nu}_{\mathrm{d}_{r;\hat{p}}}$) scanned during the processing will be suppressed. Applying the APES method implies to work with $\tilde{\boldsymbol{u}}_{i;l}$

$$\tilde{\boldsymbol{u}}_{i;l} = \mathrm{vec}(\tilde{\boldsymbol{Y}}_{i:i+M_s-1,l:l+\tilde{M}_d-1}) \tag{12}$$

and

$$\tilde{\mathrm{Y}} \triangleq [\tilde{\boldsymbol{u}}_{1;1}, \ldots, \tilde{\boldsymbol{u}}_{L_{\mathrm{s}};1}, \tilde{\boldsymbol{u}}_{1;2}, \ldots, \tilde{\boldsymbol{u}}_{L_{\mathrm{s}};\tilde{L}_{\mathrm{d}}}] \tag{13}$$

The values of M_{s}, $\tilde{M}_{\mathrm{d}}$, L_{s} and $\tilde{L}_{\mathrm{d}}$ are chosen so that $\tilde{\mathrm{Y}}$ is a square matrix ($L_{\mathrm{s}}\tilde{L}_{\mathrm{d}} = M_{\mathrm{s}}\tilde{M}_{\mathrm{d}}$). In addition, the number of antenna elements of the sparse array being small ($N_{\mathrm{s}} = 4$), M_{s} is chosen equal to N_{s} leading to $L_{\mathrm{s}} = 1$ ($L_{\mathrm{s}} = N_{\mathrm{s}} - M_{\mathrm{s}} + 1$). Once the integration time and the subsampling factor are chosen and using $\tilde{L}_{\mathrm{d}} = \tilde{N}_{\mathrm{d}} - \tilde{M}_{\mathrm{d}+1}$, we obtain

$$\tilde{M}_{\mathrm{d}} = \frac{\tilde{N}_{\mathrm{d}} + 1}{N_{\mathrm{s}} + 1} \tag{14}$$

Furthermore, we will denote $\tilde{\boldsymbol{x}}$ the first column of the matrix $\tilde{\boldsymbol{X}}^{\mathrm{T}}$. This leads us to the optimisation problem

$$\min_{\boldsymbol{h},\hat{\alpha}} \|\boldsymbol{h}^{\dagger}\tilde{\mathrm{Y}} - \hat{\alpha}(\tilde{\boldsymbol{x}}_{L_{\mathrm{s}}\tilde{L}_{\mathrm{d}}} \circ \tilde{\boldsymbol{s}}_{L_{\mathrm{s}}\tilde{L}_{\mathrm{d}}})^{\mathrm{T}}\|^2 \tag{15}$$

with the constraint

$$\boldsymbol{h}^{\dagger}(\tilde{\boldsymbol{x}}_{M_{\mathrm{s}}\tilde{M}_{\mathrm{d}}} \circ \tilde{\boldsymbol{s}}_{M_{\mathrm{s}}\tilde{M}_{\mathrm{d}}}) = 1 \tag{16}$$

$\boldsymbol{h} \in \mathbb{C}^{M_{\mathrm{s}}\tilde{M}_{\mathrm{d}}}$ is the vector containing the coefficients of the filter at the frequency $(\theta, \tilde{\nu}_{\mathrm{d}})$ for the considered range cell.

Proposition 1 (Noise APES (NAPES filter)): The solution of the optimisation problem (15) under the constraint (16) is

$$\hat{\alpha} = \boldsymbol{h}^{\dagger}\tilde{\boldsymbol{g}} \tag{17}$$

and

$$\boldsymbol{h} = \frac{\hat{\tilde{\Phi}}^{-1}\tilde{\boldsymbol{x}}^{\mathrm{sd}}_{M_{\mathrm{s}}\tilde{M}_{\mathrm{d}}}}{(\tilde{\boldsymbol{x}}^{\mathrm{sd}}_{M_{\mathrm{s}}\tilde{M}_{\mathrm{d}}})^{\dagger}\hat{\tilde{\Phi}}^{-1}\tilde{\boldsymbol{x}}^{\mathrm{sd}}_{M_{\mathrm{s}}\tilde{M}_{\mathrm{d}}}} \tag{18}$$

where

$$\tilde{\boldsymbol{g}} = \frac{1}{\|\tilde{\boldsymbol{x}}_{L_{\mathrm{s}}\tilde{L}_{\mathrm{d}}}\|^2}\tilde{\mathrm{Y}}(\tilde{\boldsymbol{x}}^{\mathrm{sd}}_{L_{\mathrm{s}}\tilde{L}_{\mathrm{d}}})^{*} \tag{19}$$

$$\hat{\tilde{\Phi}} = \frac{1}{\|\tilde{\boldsymbol{x}}_{L_{\mathrm{s}}\tilde{L}_{\mathrm{d}}}\|^2}\tilde{\mathrm{Y}}\tilde{\mathrm{Y}}^{\dagger} - \tilde{\boldsymbol{g}}\tilde{\boldsymbol{g}}^{\dagger} \tag{20}$$

$\tilde{\boldsymbol{x}}^{\mathrm{sd}}_{M_{\mathrm{s}}\tilde{M}_{\mathrm{d}}} = \tilde{\boldsymbol{x}}_{M_{\mathrm{s}}\tilde{M}_{\mathrm{d}}} \circ \tilde{\boldsymbol{s}}_{M_{\mathrm{s}}\tilde{M}_{\mathrm{d}}}$ is obtained from the reference signal, mixed, lowpass filtered, subsampled and steered in the desired spatio-temporal direction and $\|\tilde{\boldsymbol{x}}_{L_{\mathrm{s}}\tilde{L}_{\mathrm{d}}}\|^2 = L_{\mathrm{s}} \sum_{l=1}^{\tilde{L}_{\mathrm{d}}} |\tilde{x}_l|^2$.

The proof of the proposition is given in the Appendix. Range cells index r are processed one after the other. Once the Doppler, angle and amplitude of the main contributor to clutter in this range cell is estimated using the APES

IET Signal Process., 2010, Vol. 4, Iss. 3, pp. 298–304
doi: 10.1049/iet-spr.2009.0067

Table 1 Configuration parameters

Acquisition parameters							
$\tilde{N}_d$	74	N_s	4	S	2^{13}	T_{ci}	66 ms
Emitter							
EIRP	20 kW	central frequency	562 MHz				
Target							
signal-to-clutter ratio	−40 dB	direction of arrival (θ)	22°				
f_d	−30 Hz	range cell (τf_s)	50				

method, this contribution is subtracted. One obtain at iteration number p for the range cell r

$$\hat{\hat{\boldsymbol{Y}}}_t^{(r;p)} = \hat{\hat{\boldsymbol{Y}}}_t^{(r;p-1)} - \hat{\hat{\boldsymbol{Y}}}_c^{(r;p)} = \hat{\hat{\boldsymbol{Y}}}_t^{(r;p-1)} - \hat{\alpha}^{(r;p)} \boldsymbol{s}_s(\theta_{r;p})(\boldsymbol{x}(-\tau_r) \circ \boldsymbol{s}_d(\tilde{\nu}_{d_{r;p}}))^T \quad (21)$$

with $\hat{\hat{\boldsymbol{Y}}}_t^{(1;1)} = \tilde{\boldsymbol{Y}}$ and $\hat{\alpha}^{(r;p)} = \max_p \hat{\alpha}_{r;p}$.

4 Real clutter rejection using the APES method

This section presents the results obtained applying an iterative rejection thanks to the APES method to real ground clutter where a target has been injected.

Table 1 provides the configuration parameters of the measured ground clutter created by the Eiffel Tower DVB−T emitter.

One can see how efficient the iterative clutter rejection is by comparing range-Doppler map ($\max_\theta \alpha(\tau, \theta, f_d)$) before, (Fig. 1*a*) and after processing (Fig. 1*b*). The position of the target is represented by a black cross.

Figs. 2*a* and *b* offer a zoomed version of the previous figures.

The area of rejection has been chosen between range cell number 20 and range cell number 80 in order to prove the feasibility of a localised clutter rejection. This possibility can clearly be seen in Fig. 1*b*.

The data have been collected from a static receiver and the hypothesis of internal clutter motion has been made. The rejection was applied between −5 and 5 Hz and all over angles between −90° and 90°.

Fig. 3*a* focuses on the range cell 50 where the target has been injected. One can see in this figure that if the target is hidden in a sidelobe of the clutter before rejection, it appears in Fig. 3*b* after clutter rejection.

One can wonder if a lack of precision in the estimation of the amplitude of a clutter component or the rejection of a range sidelobe instead of a main contribution could lead to an unwanted increase of clutter level. The number of iterations necessary to reach the level of −16 dB, for each range cell and for four successive iterations set is presented in Fig. 4*a*. It allows to check that a single step (Fig. 4*b*) of cleaning is sufficient.

Fig. 5*a* illustrates the level after rejection as a function of the number of iterations for the first set. Fig. 5*b* shows that for the range cell number 41 where the most important number of iterations is necessary (79 iterations whereas the mean over the 59 other range cells is 17 iterations) 32 iterations are sufficient to reach the level of −13 dB corresponding to a rejection in power of 52 dB.

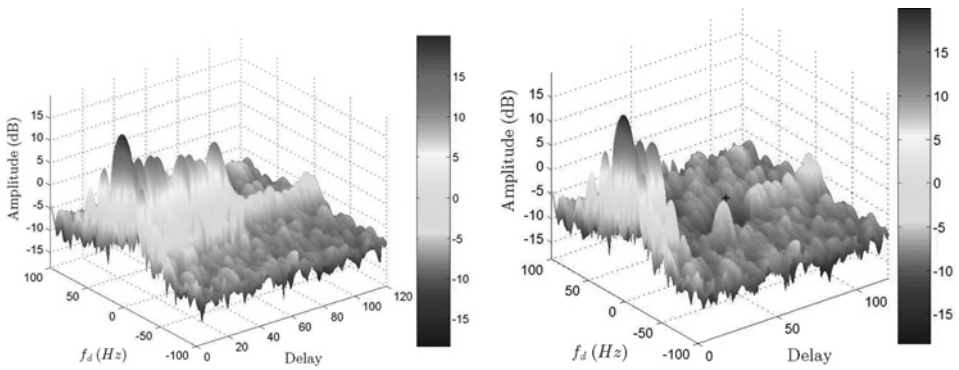

Figure 1 *Efficiency of iterative clutter rejection*

a $\max_\theta \alpha(\tau, \theta, f_d)$ before rejection
b $\max_\theta \alpha(\tau, \theta, f_d)$ after rejection

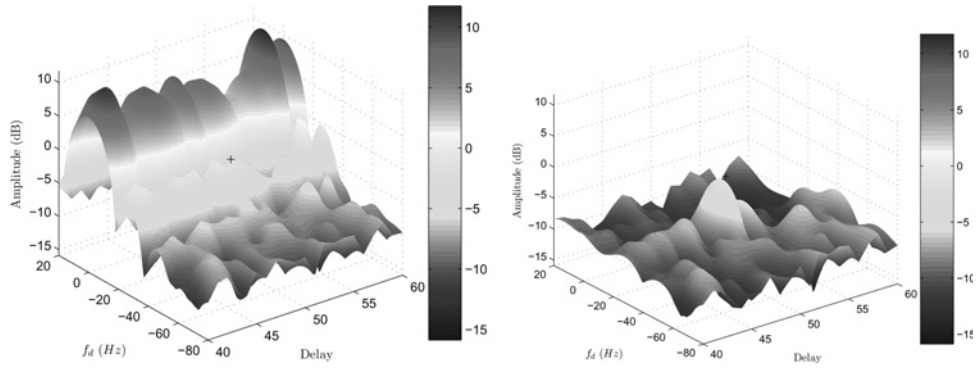

Figure 2 *Zoomed version of Figs. 1a and b*

a $\max_\theta \alpha(\tau, \theta, f_d)$ before rejection (zoom)
b $\max_\theta \alpha(\tau, \theta, f_d)$ after rejection (zoom)

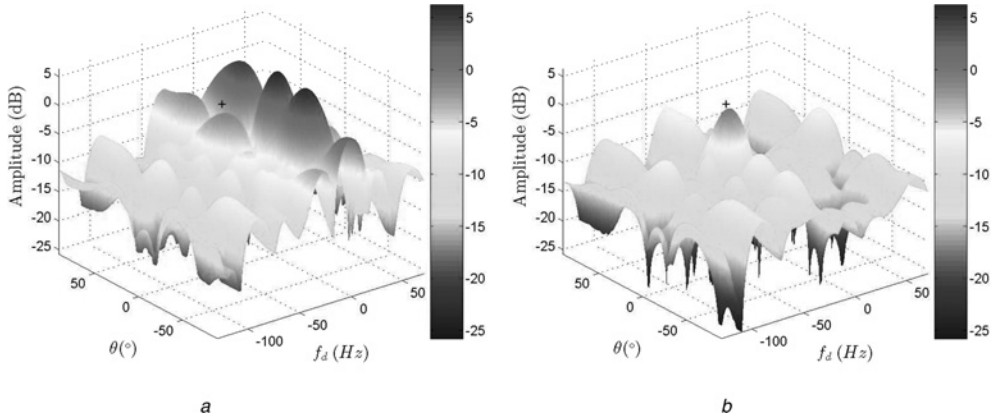

Figure 3 *Range cell 50 where the target has been injected*

a $\alpha(\theta, f_d)$ in range cell 50 before rejection
b $\alpha(\theta, f_d)$ in range cell 50 after rejection

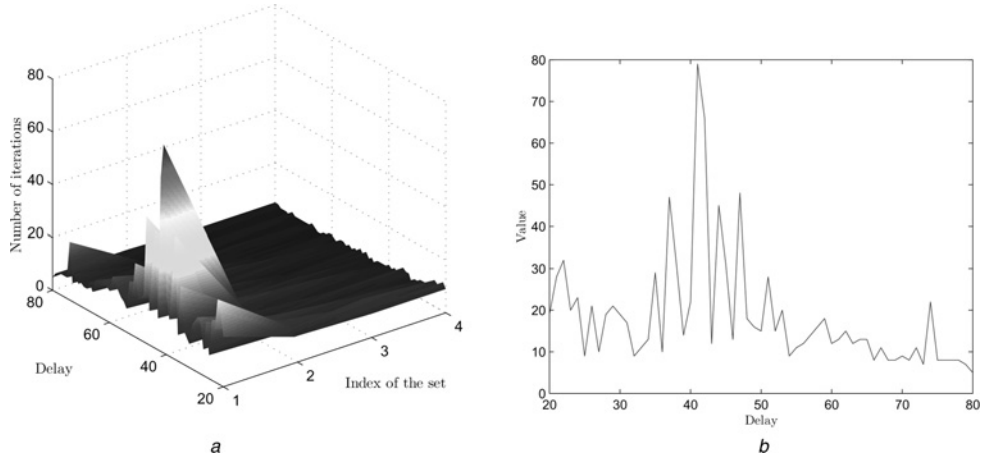

Figure 4 *Number of iterations necessary to reach −16 dB threshold*

a Each range cell and four successive iterations set
b Single step of clearing

IET Signal Process., 2010, Vol. 4, Iss. 3, pp. 298–304
doi: 10.1049/iet-spr.2009.0067

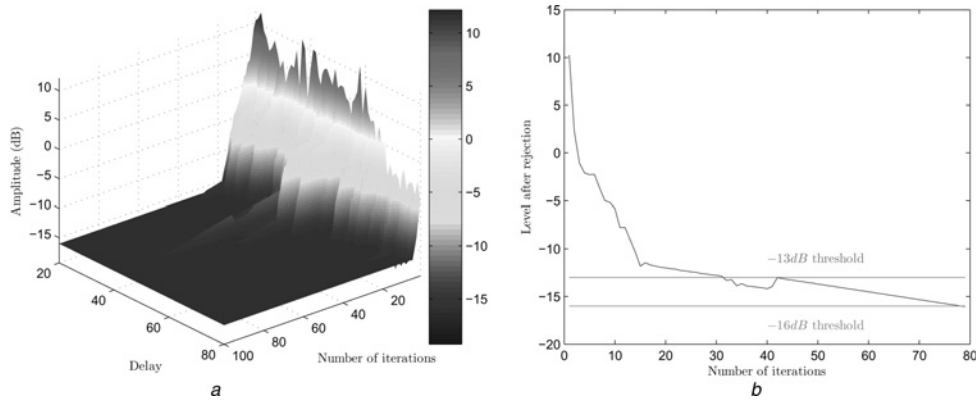

Figure 5 *Level after rejection as a function of number of iterations*

a For all range cells
b For range cell 41

5 Conclusion

We have shown in this paper how efficient the APES method could be in the frame of the rejection of real ground clutter even for a small number of iterations. The estimation of the so-called covariance matrix associated to most of the space–time adaptive processing is no longer necessary but is replaced by an iterative rejection of the main contributors to the interference, one range cell after the other. It is not fully adaptive but it needs a preliminary knowledge of the clutter power spectral density (PSD) locus either thanks to a knowledge-aided process or an initial step of estimation. It potentially suppresses the difficulties linked to a non-homogeneous environment and range dependence of the clutter PSD. This method successfully applied to a ground-based bistatic and passive scenario for a proof of feasibility should also be applicable to a moving transmitter and/or receiver for any antenna configuration.

6 Acknowledgment

The authors would like to thank François Delaveau and François Pipon (Thales-communications, EDS/SPM/SBP, Colombes, France) for providing raw data.

7 References

[1] ZHENG H., LI F., LUO J., LU J.: 'Bistatic radar experiment based on *FM* broadcast transmitter'. Proc. IEEE Radar Conf., Toulouse, France, October 2004

[2] HORNER J., KUBIK K., MOJARRABI B., LONGSTAFF I.D., DONSKOI E., CHERNIAKOV M.: 'Passive bistatic radar sensing with *LEOS* based transmitters'. Proc. IGARSS'02, Toronto, Canada, June 2002, vol. 1, pp. 438–440

[3] SAINI R., CHERNIAKOV M., LENIVE V.: 'Direct path interference suppression in bistatic system: *DTV* based radar'. Proc. Int. Radar Conf. 2003, September 2003, pp. 309–314

[4] KUBICA M., KUBICA V., NEYT X., RAOUT J., ROQUES S., ACHEROY M.: 'Optimum target detection using emitters of opportunity'. Proc. IEEE Radar Conf., Verona, NY, April 2006, pp. 417–424

[5] GRIFFITHS H.D., BAKER C.J.: 'Measurement and analysis of ambiguity functions of passive radar transmissions'. Proc. IEEE Radar Conf., Arlington, VA, May 2005, pp. 321–325

[6] KLEMM R.: 'Principles of space–time adaptive processing' (The Institution of Electrical Engineers (IEE) Press, London, UK, 2002)

[7] GUERCI J.R.: 'Space–time adaptive processing for radar' (Artech House, Norwood, MA, 2003)

[8] RAOUT J., NEYT X., RISCHETTE P.: 'Bistatic *STAP* using illuminators of opportunity'. Proc. IET Conf. on Radar Systems, Edinburgh, Scotland, 15–18 October 2007

[9] WANG H., CAI L.: 'On adaptive spatial-temporal processing for airborne surveillance radar systems', *IEEE Trans. Aerosp. Electron. Syst.*, 1994, **30**, (3), pp. 660–670

[10] RAOUT J., PRÉAUX J.P.: 'Multi-target detection using noise-like signals'. Proc. IEEE Radar Conf., Rome, Italy, 26–30 May 2008

[11] RAOUT J.: 'Space–time adaptive processing for noise-radar'. Proc. IEEE Radar Conf., Rome, Italy, 26–30 May 2008

[12] WICKS M.C., RANGASWAMY M., ADVE R., HALE T.B.: 'Space–time adaptive processing: a knowledge-based perspective for airborne radar', *IEEE Trans. Aeros. Electron. Syst.*, 2006, **23**, (1), pp. 51–65

[13] LI J., STOICA P.: 'An adaptive filtering approach to spectral estimation and SAR imaging', *IEEE Trans. Signal Process.*, 1996, **44**, (2), pp. 1469–1484

[14] STOICA P., LI H., LI J.: 'A new derivation of the APES filter', *IEEE Signal Process. Lett.*, 1999, **6**, pp. 205–206

[15] STOICA P., LI H., LI J.: 'Amplitude estimation of sinusoidal signals: survey, new results and an application', *IEEE Trans. Signal Process.*, 2000, **48**, pp. 338–352

[16] STEIN S.: 'Algorithms for ambiguity function processing', *IEEE Trans. Acoustics, Speech Signal Process.*, 1981, **29**, (3), pp. 588–599

8 Appendix

Note: In the following proof the index $_i$ will correspond to antenna elements and the index $_l$ to samples.

Temporal and spatial phase shifts are defined in Section 2.

The mixed, low-pass filtered and subsampled version of the reference signal $\tilde{\boldsymbol{x}}$, and the parameters L_{s}, $\tilde{L}_{\mathrm{d}}$, M_{s} and $\tilde{M}_{\mathrm{d}}$ are defined in Section 3. The vector $\tilde{\boldsymbol{u}}_{i,l}$ is also defined in this section in (12).

Proof: Let us consider $I(\alpha, \boldsymbol{h})$ the quantity to be optimised under constraint in order to estimate the amplitude of the target α thanks to $\boldsymbol{h} \in \mathbb{C}^{M_{\mathrm{s}}\tilde{M}_{\mathrm{d}}}$ the vector containing the coefficients of the filter at the frequency $(\theta, \tilde{\nu}_{\mathrm{d}})$ for the considered range cell:

$$
\begin{aligned}
I(\alpha, \boldsymbol{h}) &= \sum_{i=1}^{L_{\mathrm{s}}} \sum_{l=1}^{\tilde{L}_{\mathrm{d}}} \left| \boldsymbol{h}^{\dagger} \tilde{\boldsymbol{u}}_{i,l} - \alpha \tilde{x}_l \tilde{z}_{\mathrm{d}}^{l-1} \prod_{k=0}^{i-1} z_{\mathrm{s}_{k+1,k}} \right|^2 \\
&= \sum_{i=1}^{L_{\mathrm{s}}} \sum_{l=1}^{\tilde{L}_{\mathrm{d}}} \left(\boldsymbol{h}^{\dagger} \tilde{\boldsymbol{u}}_{i,l} - \alpha \tilde{x}_l \tilde{z}_{\mathrm{d}}^{l-1} \prod_{k=0}^{i-1} z_{\mathrm{s}_{k+1,k}} \right) \\
&\quad \times \left(\tilde{\boldsymbol{u}}_{i,l}^{\dagger} \boldsymbol{h} - \alpha^* \tilde{x}_l^* \tilde{z}_{\mathrm{d}}^{-(l-1)} \prod_{k=0}^{i-1} z_{\mathrm{s}_{k+1,k}}^* \right) \\
&= \boldsymbol{h}^{\dagger} \sum_{i=1}^{L_{\mathrm{s}}} \sum_{l=1}^{\tilde{L}_{\mathrm{d}}} \tilde{\boldsymbol{u}}_{i,l} \tilde{\boldsymbol{u}}_{i,l}^{\dagger} \boldsymbol{h} + \sum_{i=1}^{L_{\mathrm{s}}} \sum_{l=1}^{\tilde{L}_{\mathrm{d}}} |\alpha|^2 |\tilde{x}_l|^2 \\
&\quad - \alpha^* \boldsymbol{h}^{\dagger} \sum_{i=1}^{L_{\mathrm{s}}} \sum_{l=1}^{\tilde{L}_{\mathrm{d}}} \tilde{x}_l^* \tilde{z}_{\mathrm{d}}^{-(l-1)} \prod_{k=0}^{i-1} z_{\mathrm{s}_{k+1,k}}^* \tilde{\boldsymbol{u}}_{i,l} \\
&\quad - \alpha \sum_{i=1}^{L_{\mathrm{s}}} \sum_{l=1}^{\tilde{L}_{\mathrm{d}}} \tilde{x}_l \tilde{z}_{\mathrm{d}}^{l-1} \prod_{k=0}^{i-1} z_{\mathrm{s}_{k+1},k} \tilde{\boldsymbol{u}}_{i,l}^{\dagger} \boldsymbol{h}
\end{aligned}
$$

Let us note

$$
\hat{\tilde{\Xi}} = \frac{1}{\|\tilde{\boldsymbol{x}}_{L_{\mathrm{s}}\tilde{L}_{\mathrm{d}}}\|^2} \sum_{i=1}^{L_{\mathrm{s}}} \sum_{i=1}^{\tilde{L}_{\mathrm{d}}} \tilde{\boldsymbol{u}}_{i,l} \tilde{\boldsymbol{u}}_{i,l}^{\dagger} \tag{22}
$$

and

$$
\begin{aligned}
\|\tilde{\boldsymbol{x}}_{L_{\mathrm{s}}\tilde{L}_{\mathrm{d}}}\|^2 &= \sum_{i=1}^{L_{\mathrm{s}}} \sum_{i=1}^{\tilde{L}_{\mathrm{d}}} |\tilde{x}_l|^2 \\
&= L_{\mathrm{s}} \sum_{i=1}^{\tilde{L}_{\mathrm{d}}} |\tilde{x}_l|^2
\end{aligned} \tag{23}
$$

$$
\begin{aligned}
I(\alpha, \boldsymbol{h}) &= \|\tilde{\boldsymbol{x}}_{L_{\mathrm{s}}\tilde{L}_{\mathrm{d}}}\|^2 \boldsymbol{h}^{\dagger} \hat{\tilde{\Xi}} \boldsymbol{h} + \|\tilde{\boldsymbol{x}}_{L_{\mathrm{s}}\tilde{L}_{\mathrm{d}}}\|^2 (|\alpha|^2 - \alpha^* \boldsymbol{h}^{\dagger} \tilde{\boldsymbol{g}} - \alpha \tilde{\boldsymbol{g}}^{\dagger} \boldsymbol{h}) \\
&= \|\tilde{\boldsymbol{x}}_{L_{\mathrm{s}}\tilde{L}_{\mathrm{d}}}\|^2 (\boldsymbol{h}^{\dagger} \hat{\tilde{\Xi}} \boldsymbol{h} + |\alpha - \boldsymbol{h}^{\dagger} \tilde{\boldsymbol{g}}|^2 - |\boldsymbol{h}^{\dagger} \tilde{\boldsymbol{g}}|^2) \\
&= \|\tilde{\boldsymbol{x}}_{L_{\mathrm{s}}\tilde{L}_{\mathrm{d}}}\|^2 (\boldsymbol{h}^{\dagger} (\hat{\tilde{\Xi}} - \tilde{\boldsymbol{g}} \tilde{\boldsymbol{g}}^{\dagger}) \boldsymbol{h} + |\alpha - \boldsymbol{h}^{\dagger} \tilde{\boldsymbol{g}}|^2)
\end{aligned}
$$

is minimal for

$$
\alpha = \boldsymbol{h}^{\dagger} \tilde{\boldsymbol{g}} \tag{24}
$$

The optimal $\boldsymbol{h}$ must now be evaluated. The new optimisation problem becomes

$$
\min_{\boldsymbol{h}} \boldsymbol{h}^{\dagger} \hat{\tilde{\Phi}} \boldsymbol{h} \tag{25}
$$

under the constraint

$$
\boldsymbol{h}^{\dagger} (\tilde{\boldsymbol{x}}_{M_{\mathrm{s}}M_{\mathrm{d}}}^{\mathrm{sd}}) = 1 \tag{26}
$$

with

$$
\hat{\tilde{\Phi}} = \hat{\tilde{\Xi}} - \tilde{\boldsymbol{g}} \tilde{\boldsymbol{g}}^{\dagger} \tag{27}
$$

This quadratic optimisation problem with a linear equality constraint can be solved using Lagrange multipliers. The solution (when it exists) is

$$
\boldsymbol{h} = \frac{\hat{\tilde{\Phi}}^{-1} \tilde{\boldsymbol{x}}_{M_{\mathrm{s}}\tilde{M}_{\mathrm{d}}}^{\mathrm{sd}}}{(\tilde{\boldsymbol{x}}_{M_{\mathrm{s}}\tilde{M}_{\mathrm{d}}}^{\mathrm{sd}})^{\dagger} \hat{\tilde{\Phi}} \tilde{\boldsymbol{x}}_{M_{\mathrm{s}}\tilde{M}_{\mathrm{d}}}^{\mathrm{sd}}} \tag{28}
$$

This last equation, in association with (24), provides the optimal solution. □

doi: 10.1049/iet-spr.2009.0067